Effects of nanoparticle-mediated delivery of pitavastatin on atherosclerotic plaques in ApoE-knockout mice and THP-1-derived macrophages

YUJIAO SUN, LING CHEN, SHIJIE ZHAO, LIYE SHI, HUA LI, WEN TIAN and GUOXIAN QI

Department of Geriatric Cardiology, The First Affiliated Hospital of China Medical University,
Shenyang, Liaoning 110001, P.R. China

Abstract. The treatment of atherosclerosis remains complex. Pitavastatin serves an important role in the prevention and treatment of atherosclerosis. The present study aimed to investigate the effects of nanoparticle (NP)-mediated delivery of pitavastatin into atherosclerotic plaques as a novel treatment method for atherosclerosis. The results of the present study demonstrated that pitavastatin-NP was more effective in attenuating the size of atherosclerotic plaques and enhancing the stability of plaques *in vitro* compared with pitavastatin alone. In an apolipoprotein E (ApoE)-knockout mouse model of atherosclerosis, a single intravenous injection of fluorescein isothiocyanate-NP resulted in the delivery of NP into atherosclerotic plaques for up to 7 days post-injection. In ApoE-knockout mice and THP-1-derived macrophages, pitavastatin-NP attenuated the development of atherosclerosis, which was associated with regulating lipid metabolism, and inhibited the secretion of inflammatory markers compared with pitavastatin alone. Additionally, the treatment advantages of pitavastatin-NP were independent of lipid lowering. The results demonstrated that pitavastatin-NP administration was more effective in attenuating the development of atherosclerotic plaques compared with systemic administration of pitavastatin.

Introduction

Atherosclerosis is one of the leading cause of death worldwide (1). Atherosclerotic plaques are difficult to reverse once formed; however, statins are regarded as the most effective drugs for the prevention of atherosclerotic plaque formation (1).

Correspondence to: Dr Guoxian Qi, Department of Geriatric Cardiology, The First Affiliated Hospital of China Medical University, 155 Nanjing North Street, Shenyang, Liaoning 110001, P.R. China
E-mail: qiguoxiantg@163.com

Numerous studies have reported that statins can reduce the plaque volume following prolonged high-dose statin administration (2-4). However, these studies have also demonstrated that the reduction in the plaque volume was limited despite long-term treatment with high doses of statins (2-4), making statins an unsatisfactory solution to the global demand for clinical treatment.

A novel drug delivery system (DDS) has been established using nanoparticle (NP)-mediated approaches. NPs are biodegradable copolymers that change the pharmacokinetic properties of drugs *in vivo* and increase the distribution of drugs in organs (5). The NP-DDS can enhance the efficacy and safety of therapeutic agents and overcome numerous drawbacks of the agents such as toxicity, low water solubility, poor bioavailability and low organ specificity (5). Previous studies have demonstrated that pitavastatin inhibits pulmonary artery smooth muscle cell proliferation more effectively compared with other statins, including rosuvastatin, pravastatin, simvastatin, atorvastatin and lovastatin (6), which might explain that pitavastatin has advantages over other statins in preventing atherosclerosis. Pitavastatin-NP (P-NP) has exhibited significant advantages in experimental studies of angiogenesis in ischemic tissue (7,8) and in the prevention and treatment of pulmonary hypertension (6). These effects may result primarily from the efficiency and durability of the NP-DDS, as well as its ability to target the location of the lesion. Additionally, pitavastatin-incorporated NP-eluting stents were reported to attenuate in-stent stenosis without delayed endothelial healing effects in a porcine coronary artery model (9). Administration of P-NP is frequently used in experimental studies and its theory and technology are well understood (6-9). Therefore, P-NP was used in the present study.

A limited number of reports have focused on the effects of P-NP on atherosclerotic plaques. The present study aimed to examine whether administration of P-NP may inhibit the progression of atherosclerotic plaques and to elucidate its mechanism of action.

Materials and methods

Preparation of nanoparticles. Lactide/glycolide copolymer (PLGA) with a copolymer ratio of lactide to glycolide of

75:25 was used for the NP. PLGA nanoparticles encapsulated with FITC (FITC-NP) and P-NP were constructed using an emulsion solvent diffusion method as previously described (6). The FITC-loaded NP contained 4.06% (wt/vol) FITC, and the pitavastatin-loaded NP contained 12% (wt/vol) pitavastatin.

Animal preparation and experimental protocol. The study was approved by The Institutional Animal Care and Use Committee, China Medical University (Shenyang, China). C57BL/6J apolipoprotein E (ApoE)-knockout mice (n=60, male, 8-week-old, 20-30 g) were purchased from Beijing Vital River Laboratory Animal Technology Co. Ltd. The mice were housed at a constant temperature (20-22°C) and humidity (40-50%) with a 12-h light/dark cycle and received a high-fat diet and tap water to establish the atherosclerosis model; the high-fat diet (0.2% cholesterol, 21.2% fat, 13.7% saturated fatty acids, 7.3% total unsaturated fatty acids; Harlan Teklad; cat. no. TD.88137) was maintained throughout the experiment. The well-being of the mice was monitored during the experimental period by assessing their physical characteristics, activity, behavior, weight and reactions to external stimuli. The humane endpoints were defined as 10-20% weight loss, impaired ambulation preventing the animals from reaching food or water, lack of physical or mental alertness, abnormal breathing and prolonged inability to remain upright.

A total of 48 ApoE-knockout mice were randomly divided into six groups (n=8 mice/group): i) Control group, in which the mice were not treated; ii) PBS group, in which the mice received intravenous injections of 0.1 ml PBS once a week via the tail vein; iii) NP group, in which the mice received intravenous injections of NP equivalent to the NP of 0.4 mg/kg P-NP once a week via the tail vein [the P-NP contained 88% (wt/vol) NP]; iv) P-IV group, in which the mice received an intravenous injection of 0.4 mg/kg pitavastatin once a week via the tail vein; v) P-NP group, in which the mice received an intravenous injection of P-NP containing 0.4 mg/kg (7) pitavastatin at once a week via the tail vein; and vi) P-Oral group, in which the mice were orally administered 1 mg/kg pitavastatin once a day. The mice were allowed free access to high-fat food and tap water throughout the 12-week period. The cumulative effect of intravenous P-NP was calculated using the following formula: P-NP group: Cumulative dose=20,000 mg/animal x 0.4 mg/kg/day x 12 days=96,000 mg/animal; P-Oral group: Cumulative dose=20,000 mg/animal x 1 mg/kg/day x 84 days=1,680,000 mg/animal); Cumulative effect=the cumulative dose of the P-Oral group/the cumulative dose of the P-NP group.

The mice were then euthanized by an intraperitoneal injection of 150 mg/kg sodium pentobarbital. Death was verified by the absence of a corneal reflex, respiration and heartbeat. Subsequently, the midline of the mouse abdomen was incised, and the thorax was opened to expose the heart and aorta. The aorta was dissected out between the aortic root and the abdominal aorta, and the fat and connective tissues were removed with fine forceps.

Oil Red O staining of atherosclerotic plaques. The mouse aortas were completely separated, and the aorta strips were fixed with fine needles on a black rubber sheet. The aorta strips were placed in PBS for 2 min at room temperature and subsequently differentiated in a mixture of 60% isopropanol in distilled water for 1 min at room temperature, incubated in Oil Red O solution (cat. no. O8010; Beijing Solarbio Science and Technology Co., Ltd) for 10 min at room temperature, differentiated in a mixture of 60% isopropanol in distilled water for a further 2 min at room temperature, and finally rinsed in PBS for 2 min at room temperature. The stained aorta strips were imaged, and the Oil Red O-positive area and total luminal surface area from the aortic root to the abdominal aorta were measured using an SZX16 stereoscopic microscope (Olympus Corporation; magnification x3).

Distribution and persistence of FITC-NP. Following 12-week high-fat diet administration, six randomly selected mice received 0.4 mg/kg FITC-NP and another six randomly selected mice received 0.4 mg/kg FITC through an intravenous injection into the tail vein. The mice were euthanized 1 or 7 days post-injection (four groups: FITC 1 day, FITC-NP 1 day, FITC 7 days and FITC-NP 7 days; n=3 mice/group). The aortas were dissected, frozen using optimal cutting temperature compound (cat. no. 4583; Sakura Finetek USA, Inc.) and stored at -20°C. Serial cross-sections of 5 μm were made using a microtome at one side on the aortic root. The nuclei were counterstained with DAPI (blue) at room temperature for 3 min. Fluorescence distribution in atherosclerotic plaques was observed under a fluorescence microscope (Olympus Corporation; magnification, x200 and x400).

Histological and immunohistochemical analysis. The aortic was removed, fixed with 4% paraformaldehyde for 24 h and embedded in paraffin at room temperature. Histological and immunohistochemical evaluation was performed to evaluate the stability of atherosclerotic plaques in 5-μm paraffin-embedded sections from the dissected aortic roots from the control, PBS, NP, P-IV, P-Oral and P-NP groups. The cross-sections of aortic roots were stained with anti-mouse Mac-3 (Mac-3; 1:200; cat. no. 550292; BD Pharmingen; BD Biosciences) and α-smooth muscle actin (α-actin; 1:50; cat. no. sc-32251; Santa Cruz Biotechnology, Inc.) primary antibodies overnight at 4°C, followed by incubation with peroxidase-conjugated goat anti-rat immunoglobulin G (IgG; 1:1,000; cat. no. zb2307; Zhongshan Jinqiao Biotechnology Co., Ltd) or peroxidase-conjugated goat anti-mouse IgG (1:1,000; cat. no. zb2305; Zhongshan Jinqiao Biotechnology Co., Ltd.) for another 30 min at room temperature. The nuclei were counterstained with hematoxylin at room temperature for 2 min. The images of five microscopic fields from three different sections from each animal were obtained using a light microscope (Olympus Corporation; magnification, x200). The positive staining integrated optical density (IOD) value was measured by Image-Pro Plus 6.0 color microscopic image analysis software (Media Cybernetics, Inc.) for semi-quantitative analysis.

Cell culture. The human monocyte cell line THP-1 was purchased from The Shanghai institutes for Biological sciences. THP-1 cells were cultured in RPMI-1640 medium (Thermo Fisher Scientific, Inc.) containing 10% fetal bovine serum (FBS; GE Healthcare Life Sciences), 100 U/ml penicillin and 100 U/ml streptomycin in a humidified atmosphere
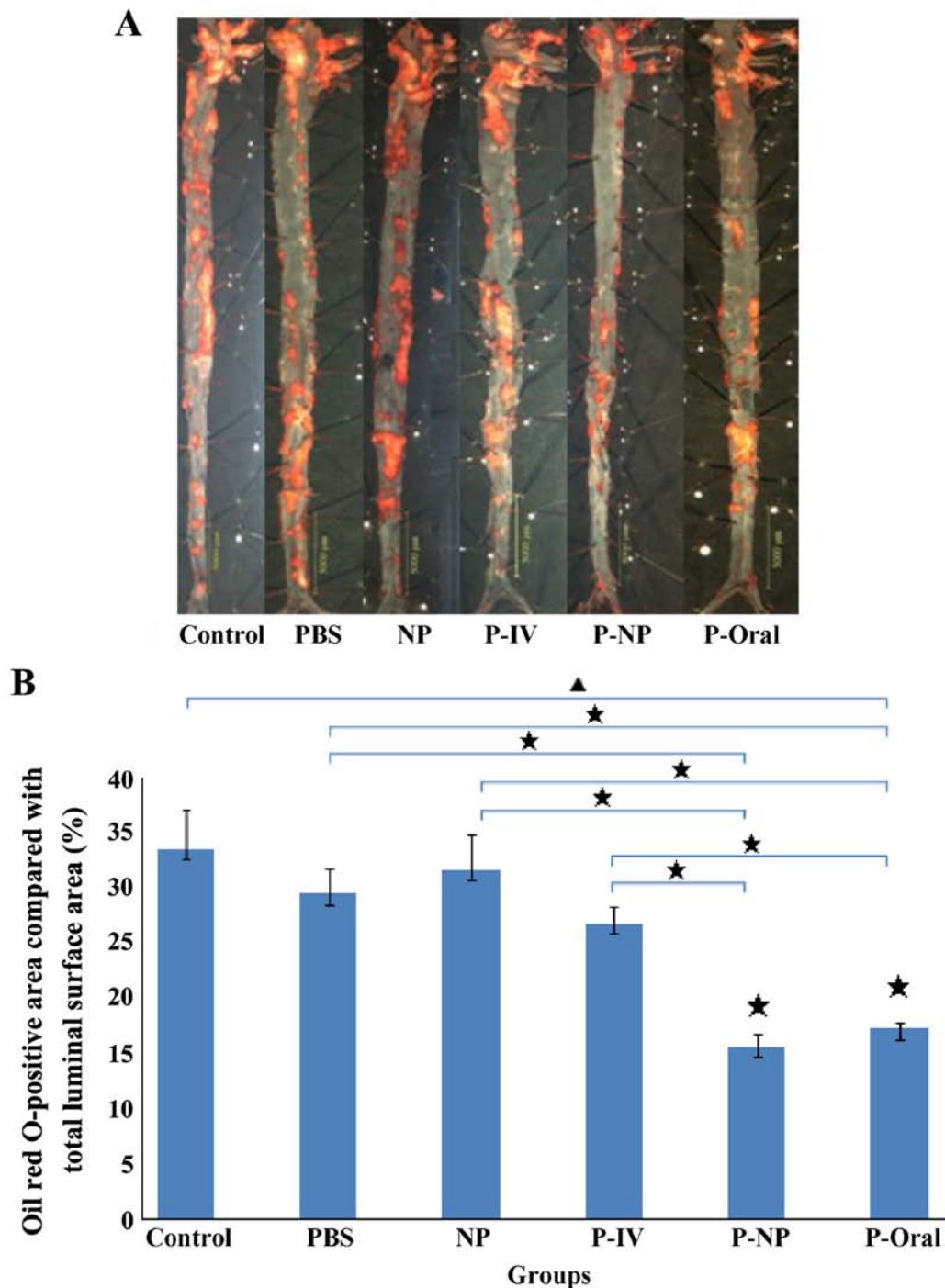
Figure 1. Oil Red O-positive areas compared with total luminal surface areas among the study groups. (A) The atherosclerotic plaques of aortas were determined by Oil Red O staining. Scale bar, 5 mm. (B) Effects of P-NP on the percentages of Oil Red O-positive areas (% total luminal surface area) in ApoE-knockout mice. [▲]P<0.05 among all groups; [★]P<0.05 vs. control or as indicated. n=4. NP, nanoparticle; P-IV, pitavastatin intravenous; P-NP, pitavastatin nanoparticle; P-Oral, pitavastatin oral.

with 5% CO_2 at 37˚C. THP-1 cells have been demonstrated to differentiate into macrophages following stimulation with phorbol-12-myristate-13-acetate (PMA) (10). THP-1 cells were seeded in 6-well culture plates at $1x10^6$ cells/ml and stimulated with 100 ng/ml PMA (cat. no. P1585; Sigma-Aldrich; Merck KGaA) for 48 h to obtain adherent macrophages. Differentiated cells exhibited macrophage-like phenotypes, which were characterized by their morphology and increased cell surface expression of CD11b by flow cytometry analysis (Fig. S1) as described in a previous study (10). THP-1 macrophages were

used in the subsequent experiments. THP-1 macrophages were incubated with 50 μg/ml oxidized low-density lipoprotein (Beijing Xiesheng Biotechnology Co., Ltd.) for 48 h to induce foam cell formation. FBS-free RPMI-1640 medium was subsequently used.

A 1.0 ml suspension of 0.5 mg/ml pitavastatin, 0.5 mg/ml NP, P-NP containing 0.5 mg/ml pitavastatin or vehicle was added to each well (n=6). After 1 h, the cells were washed three times with PBS, incubated for another 7 days and collected for future analysis.

Western blotting. The key enzymes of lipid metabolism regulation in macrophages were evaluated by immunoblotting. The whole aortas of the ApoE-knockout mice were isolated and collected. The frozen samples were homogenized in RIPA lysis buffer (Beyotime Institute of Biotechnology), and the protein concentration was measured using the BCA Protein Assay Kit (Thermo Fisher Scientific, Inc.). A total of 500-700 µg of protein was extracted from each aorta. The proteins (20 µg/lane) were separated on 7.5% SDS-polyacrylamide gels, blotted to polyvinylidene fluoride membranes, blocked with 5% skim milk for 1 h at room temperature and incubated with scavenger receptor-A1 (SR-A1; 1:500; cat. no. S3195; Sigma-Aldrich; Merck KGaA) and cholesterol acyltransferase 1 (ACAT-1; 1:300; cat. no. sc-161307; Santa Cruz Biotechnology, Inc.) antibodies overnight at 4°C. The membranes were then washed with TBS-Tween-20 and incubated with the appropriate horseradish peroxidase-linked secondary antibody goat anti-rabbit IgG (1:1,000; cat. no. zb2301; Zhongshan Jinqiao Biotechnology Co., Ltd.) or peroxidase-conjugated rabbit anti-goat IgG (1:1,000; cat. no. zb2306; Zhongshan Jinqiao Biotechnology Co., Ltd.), for 1 h at room temperature with gentle agitation, and the immune complexes were detected by enhanced chemiluminescence (ECL) using an ECL kit (Thermo Fisher Scientific, Inc.). Densitometric analyses were performed using ImageJ 1.44 software (National Institutes of Health) and normalized to the loading control protein β-actin (1:1,000; cat. no. TA-09; Zhongshan Jinqiao Biotechnology Co., Ltd.).

ELISA. Blood samples were collected from the left ventricles of the mice by heart puncture prior to euthanasia. The samples were placed in heparin containing tubes and centrifuged at 4°C at 2,000 x g for 10 min. The plasma was collected and stored at -80°C. The protein levels of total cholesterol (TC), triglyceride (TG), low density lipoprotein cholesterol (LDL-C), high density lipoprotein cholesterol (HDL-C), creatine kinase-MB (CK-MB) and alanine transaminase (ALT) in the plasma of the mice were measured by ELISA kits according to the manufacturer's instructions (cat. nos.: TC, 201-02-0614; TG, 201-02-0376; LDL-C, 201-02-0333; HDL-C, 201-02-0332; CK-MB, 201-02-0308; ALT, 201-02-0495; Shanghai Shanghong Biotechnology Co., Ltd.).

To measure the content of cholesterol ester (CE) in THP-1-derived macrophages, CE levels were analyzed using commercial reagents (cat. no. JL19339; Shanghai Future Industry Co., Ltd.). The levels of the inflammatory parameters interleukin-6 (IL-6) and tumor necrosis factor-α (TNF-α) were analyzed using ELISA kits (cat. nos.: IL-6, 201-12-0091; TNF-α, 201-12-0083; Shanghai Shanghong Biotechnology Co., Ltd.) according to the manufacturer's instructions. Absorbance was detected with a microplate reader at 450 nm for all kits.

Reverse transcription-quantitative PCR (RT-qPCR). RT-qPCR was used to assess the impact of P-NP on the expression of inflammatory factors *in vivo*. The aortas of ApoE-knockout mice were isolated and collected. Total RNA was extracted from the aortas using TRIzol® reagent (Invitrogen; Thermo Fisher Scientific, Inc.). The RNA concentration was measured by NanoDrop ND-1000 (NanoDrop Technologies; Thermo Fisher Scientific, Inc.). cDNA was synthesized at 37°C for
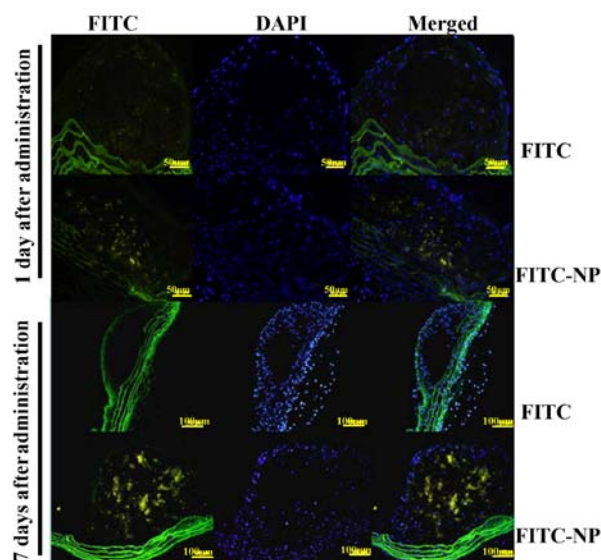

Figure 2. Localization of FITC-NP in atherosclerotic plaques of ApoE-knockout mice. Fluorescence micrographs of cross-sections from atherosclerotic plaques after intravenous injection of FITC alone or FITC-NP on days 1 and 7 after injection. The nuclei were counterstained with DAPI. n=3; scale bar, 50 and 100 µm. FITC-NP, nanoparticles encapsulated with FITC; ApoE, apolipoprotein E.

15 min followed by 85°C for 5 sec using the PrimeScript™ RT reagent (Takara Bio, Inc.). PCR amplification with the SYBR PrimeScript RT-PCR kit (Takara Bio, Inc.) was performed using an ABI PRISM 7500 Sequence Detection System (Applied Biosystems; Thermo Fisher Scientific, Inc.). The thermocycling conditions were 30 sec at 95°C, followed by 40 cycles of 5 sec at 95°C and 34 sec at 60°C. TaqMan primer sequences (Takara Biotechnology Co., Ltd.) used for RT-qPCR were as follows: Monocyte chemotactic protein 1 (MCP-1) forward, 5'-AGCAGCAGGTGTCCCAAAGA-3' and reverse, 5'-GTGCTGAAGACCTTAGGGCAGA-3'; macrophage colony-stimulating factor (M-CSF) forward, 5'-ACCACTACC CTCTCCTACCATCTTC-3' and reverse, 5'-CATCCTCCA GCCCTTTCTCTT-3'; and GAPDH forward, 5'-GGTTGT CTCCTGCGACTTCA-3' and reverse, 5'-TGGTCCAGGGTT TCTTACTCC-3'. GAPDH served as the internal reference gene. Normalization and fold-changes were calculated using the $2^{-\Delta\Delta Cq}$ method (11).

Statistical analysis. All data are presented as the mean ± standard deviation values from at least four independent experiments. Statistical analysis was performed by one-way ANOVA followed by Tukey's post-hoc test. SPSS 20.0 (IBM Corp.) was used for statistical analysis. P<0.05 was considered to indicate a statistically significant difference.

Results

Effects of P-NP on aorta plaque size. The Oil Red O-positive area compared with the total luminal surface area in ApoE-knockout mice indicated the area percentage of plaques (Fig. 1A). The percentages of the Oil Red O-positive area as follows: Control, 33.6±3.57%; PBS, 29.5±2.26%; NP, 31.7±3.2%; P-IV, 26.9±1.55%; P-NP, 15.7±1.08% and P-Oral, 17.3±0.56%
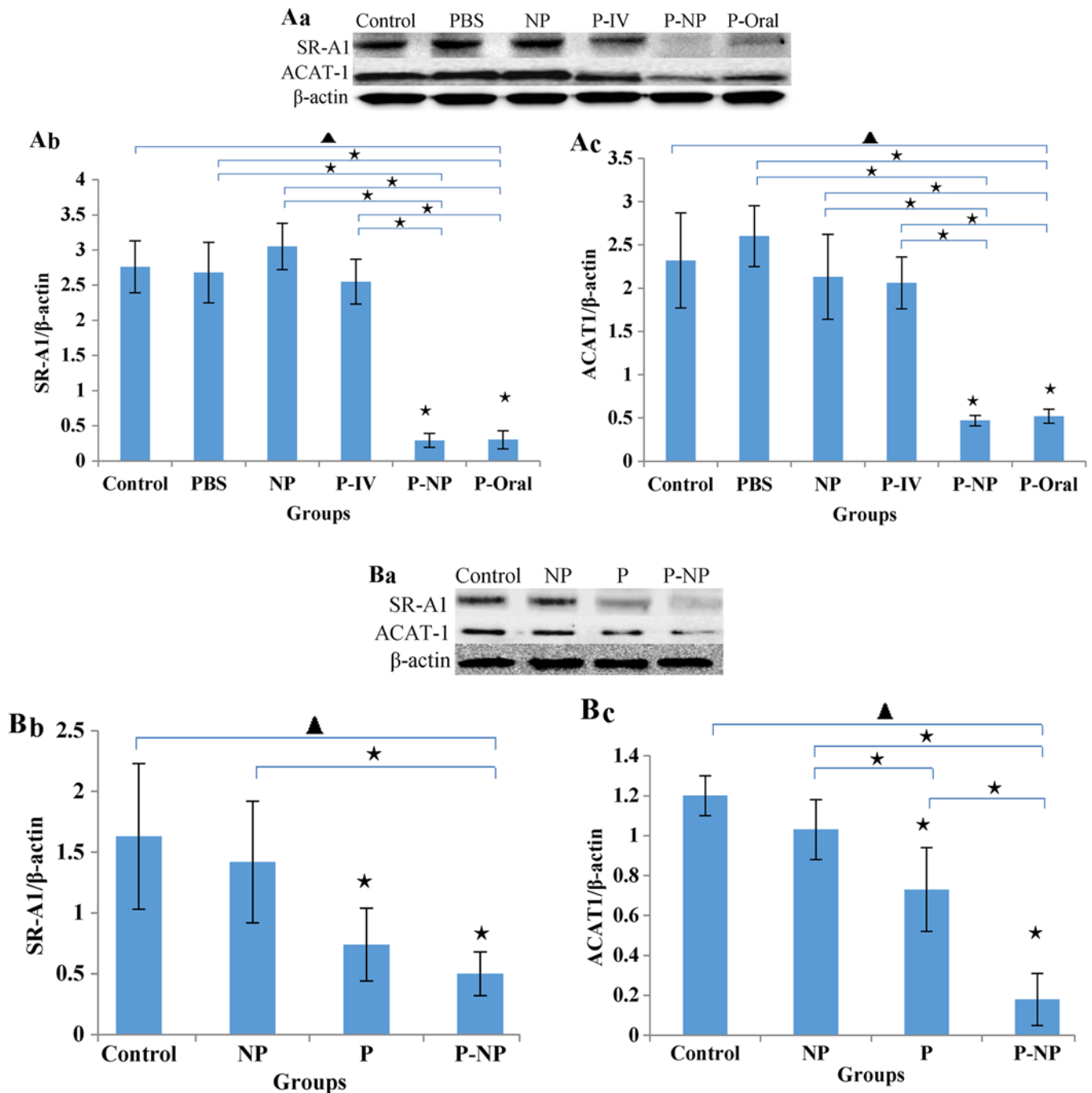
Figure 3. Effects of P-NP on regulation of lipid metabolism. (A) Effects of P-NP on SR-A1 and ACAT-1 protein secretion in ApoE-knockout mice. (A-a) SR-A1 and ACAT-1 protein secretion in ApoE-knockout mice. (A-b) The SR-A1 level is presented as a percentage of the β-actin level (n=4). (A-c) The ACAT-1 level is presented as a percentage of the β-actin level (n=4). (B) Effects of P-NP on SR-A1 and ACAT-1 protein levels in THP-1-derived macrophages. (B-a) SR-A1 and ACAT-1 protein levels in THP-1-derived macrophages. (B-b) The SR-A1 level is presented as a percentage of the β-actin level (n=6). (B-c) The ACAT-1 level is presented as a percentage of the β-actin level (n=6). Before the first antibody staining, the three protein bands were excised according to their molecular weight. The protein bands were incubated with different antibodies and exposed to X-ray film; thus, although the blot images each of these figures were from the same membrane, there was variability among each set of images. ▲P<0.05 among all groups; ★P<0.05 vs. control or as indicated. NP, nanoparticle; P-IV, pitavastatin intravenous; P-NP, pitavastatin nanoparticle; P-Oral, pitavastatin oral; SR-A1, scavenger receptor-A1; ACAT-1, cholesterol acyltransferase 1; ApoE, apolipoprotein E.

(n=4 mice/group). Significant differences were observed in the percentages of the Oil Red O-positive areas among the groups, and this percentage was significantly lower in the P-Oral and P-NP groups compared with the other groups (Fig. 1B).

Localization of FITC-NP in the atherosclerotic plaques. The localization of FITC was analyzed after a single tail vein administration of FITC-NP in ApoE-knockout mice. On day 1 after injection, stronger FITC signals were detected in the plaques of FITC-NP-injected mice compared with FITC-injected mice (Fig. 2). On day 7 post-injection, the observations were similar, with strong FITC signals detected in plaques formed in the FITC-NP-injected mice and very low FITC signals observed in the FITC-injected mice (Fig. 2). These results indicated that FITC signals were localized in the plaques of aortas for 7 days post-injection with FITC-NP.
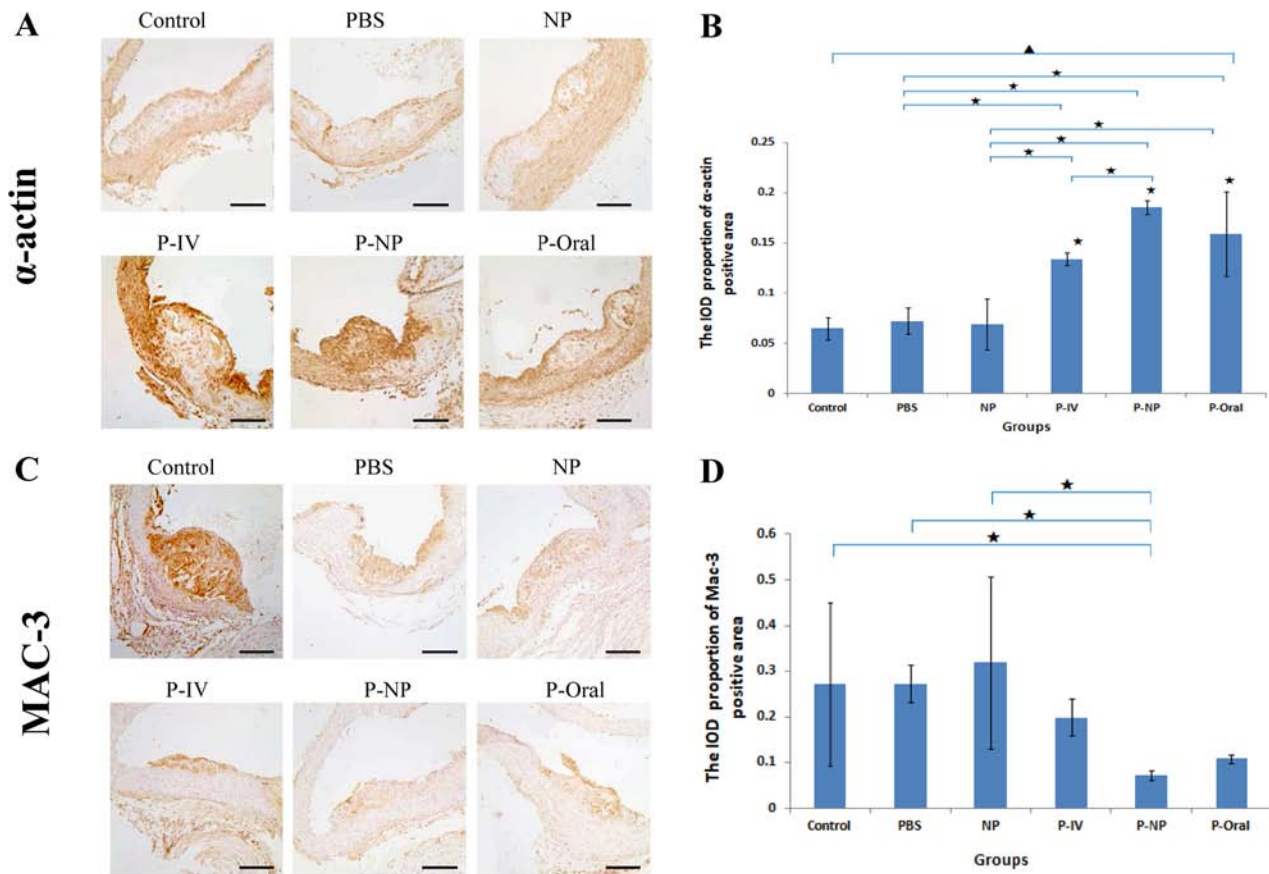
Figure 4. Effects of P-NP on the expression levels of α-actin and Mac-3 in atherosclerotic plaques of aortas. (A) Photomicrographs of cross sections of aortic roots immunohistochemically stained with α-actin. (B) Effects of P-NP on the α-actin-positive area (n=4). (C) Photomicrographs of cross-sections of aortic roots immunohistochemically stained with Mac-3. (D) Effects of P-NP on the Mac-3-positive area (n=4). Scale bar, 100 µm. ▲P<0.05 among all groups; ⋆P<0.05 vs. control or as indicated. Mac-3, Macrophage-3; PBS, phosphate-buffered saline; NP, nanoparticle; P-IV, pitavastatin intravenous; P-NP, pitavastatin nanoparticle; P-Oral, pitavastatin oral.; SR-A1, scavenger receptor-A1; ACAT-1, cholesterol acyltransferase 1; IOD, integrated optical density.

Effects of P-NP on lipid metabolism regulation. The *in vivo* protein levels of SR-A1 and ACAT-1 in the P-NP and P-Oral groups were significantly lower compared with the other groups. No significant difference was observed between the P-NP and P-Oral groups, but the levels of SR-A1 and ACAT-1 were slightly lower in the P-NP compared with the P-Oral group (Fig. 3A). The *in vitro* protein levels of ACAT-1 and SR-A1 were lower in the P-NP group compared with the control and NP groups. Additionally, the ACAT-1 level was significantly lower in the P-NP group compared with the P group (Fig. 3B).

Effects of P-NP on the stability of atherosclerotic plaques. Histological and immunohistochemical analysis revealed significant differences in the α-actin expression in atherosclerotic plaques among all groups (Fig. 4). The IOD proportion of the α-actin positive area [IOD (sum)/area (sum)] was significantly higher in the P-NP group compared with that in the control, PBS, NP and P-IV groups (Fig. 4A and B). No significant differences were observed in Mac-3 expression in atherosclerotic plaques among the groups; however, the IOD proportion of the Mac-3-positive area was significantly lower in the P-NP group compared with the control, PBS and NP groups (Fig. 4C and D). These results indicated that P-NP significantly increased the stability of atherosclerotic

plaques by increasing the expression of α-actin and reducing the expression of Mac-3.

Effects of P-NP on ALT, CK-MB and lipid levels in the ApoE-knockout mice and CE in THP-1-derived macrophages. ELISA results demonstrated that the ALT level was significantly lower in the P-NP group compared with that in the P-oral group (Fig. 5A) and that the CK-MB level was lower in the P-NP group compared with the P-Oral group, although this was not statistically significant (Fig. 5B). Additionally, no significant difference was observed in the TG, TC or HDL-C levels between the P-NP and the other groups (Fig. 5C, D and F). The LDL-C level was significantly lower in the P-IV, P-NP and P-Oral groups compared with the control group; however, there were no significant differences in the LDL-C level among the P-IV, P-NP and P-Oral groups (Fig. 5E). In THP-1-derived macrophages, the CE level was significantly lower in the P-NP group compared with the control group (Fig. 5G). The results suggested that P-NP could reduce the adverse drug reactions and P-NP has no advantage in terms of regulating lipid levels.

Effects of P-NP on the expression of inflammatory factors. The *in vivo* mRNA expression levels of MCP-1 and M-CSF were
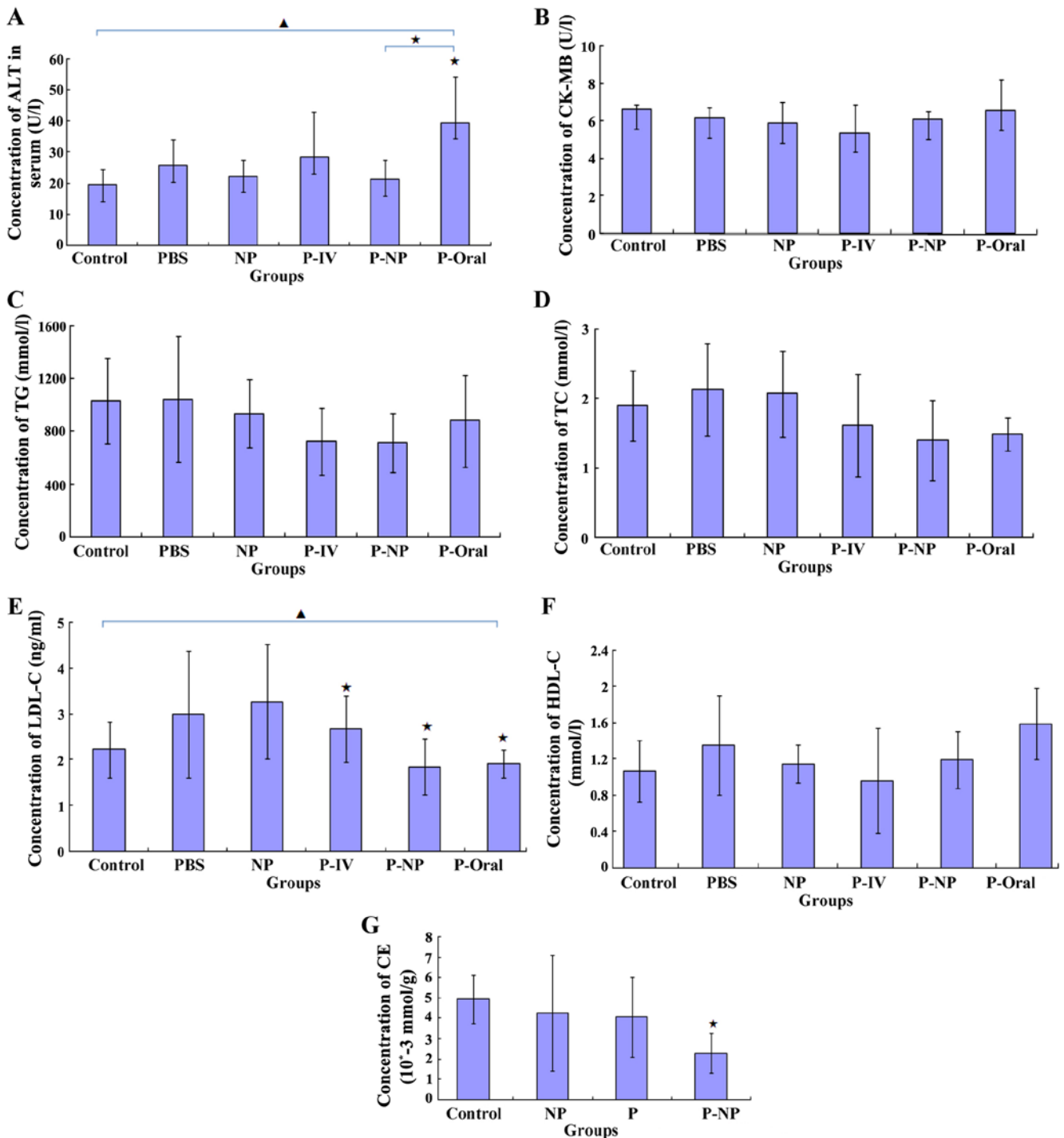
Figure 5. Effects of P-NP on biochemical parameters. (A-F) Effects of P-NP on the levels of (A) ALT, (B) CK-MB, (C) TG, (D) TC, (E) LDL-C, (F) HDL-C in the serum of the ApoE-knockout mice (n=6). (G) The effects of P-NP on the levels of intracellular CE in THP-1-derived macrophages (n=6). ▲P<0.05 among all groups; ★P<0.05 vs. control or as indicated. ALT, alanine transaminase; CK-MB, creatine kinase-MB; TG, triglyceride; TC, total cholesterol; HDL-C, high density lipoprotein cholesterol; LDL-C, low density lipoprotein cholesterol; CE, cholesterol ester; PBS, phosphate-buffered saline; NP, nanoparticle; P-IV, pitavastatin intravenous; P-NP, pitavastatin nanoparticle; P-Oral, pitavastatin oral.; SR-A1, scavenger receptor-A1; ACAT-1, cholesterol acyltransferase 1; ApoE, apolipoprotein E.

significantly lower in the P-NP and P-oral groups compared with those in the control, PBS and NP groups. Additionally, the mRNA expression levels of M-CSF and MCP-1 were lower in the P-NP group compared with the P-oral group (Fig. 6A and B). The *in vitro* protein expression of TNF-α and IL-6 was significantly lower in the P-NP group compared with the control group (Fig. 6C and D). P-NP significantly reduced the expression of inflammatory factors *in vivo* and *in vitro*.

Discussion

NP-DDS can be identified and swallowed by the mononuclear phagocyte system (including monocytes, macrophage and neutrophils), affecting the tissue/cell distribution and half-life of drugs delivered by NP-DDS (12-14). The current study demonstrated that NP carrier systems delivered pitavastatin in a site-specific manner to atherosclerotic plaques and that
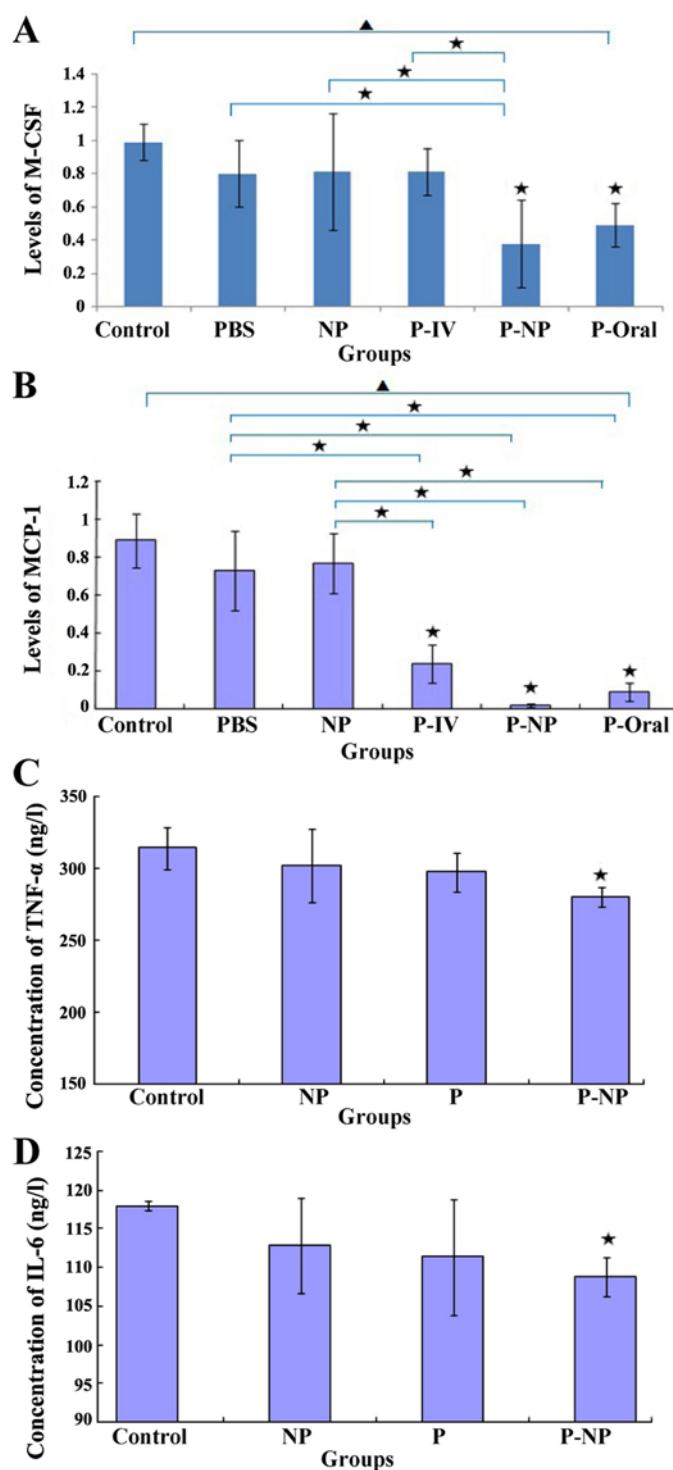
Figure 6. Effects of P-NP on M-CSF and MCP-1 mRNA and TNF-α and IL-6 protein levels. (A and B) The effects of P-NP on the mRNA levels of (A) M-CSF and (B) MCP-1 in ApoE-knockout mice (n=4). (C and D) The effects of P-NP on the protein levels of (C) TNF-α and (D) IL-6 in THP-1-derived macrophages (n=6). ▲P<0.05 among all groups; ★P<0.05 vs. control or as indicated. NP, nanoparticle; P-NP, pitavastatin nanoparticle; M-CSF, macrophage colony-stimulating factor; MCP-1, monocyte chemotactic protein 1; TNF-α, tumor necrosis factor-α; IL-6, Interleukin-6; ApoE, apolipoprotein E.

a fluorescent FITC signal was localized in atherosclerotic plaques for up to 7 days after a single intravenous injection of FITC-NP into ApoE-knockout mice. The results of the present study indicated that intravenous injection of low doses of P-NP reduced the size of atherosclerotic plaques and enhanced their stability, and reduced the ALT and CK-MB levels in the blood. In addition, P-NP regulated lipid metabolism and inhibited inflammatory reactions in THP-1 macrophages, exhibiting a significantly enhanced effect compared with pitavastatin alone. These effects were determined to be equal to or better than those resulting from a high dose of pitavastatin administered orally in ApoE-knockout mice; additionally, P-NP was demonstrated to be safer compared with large oral doses of pitavastatin.

The effects of statins on arteriosclerosis are mainly lipid-lowering and pleiotropic effects independent of lipid lowering (15). A number of clinical trials have demonstrated that

long-term and high-dose application of statins can decelerate the progression of atherosclerosis; however, the way in which statins are used can increase the risk of adverse effects and costs of medical treatment, thus reducing compliance with this medication (16,17). Therefore, in practical clinical applications, the prolonged use of high doses of statins has limitations. In recent years, NP-DDSs have been the focus of increasing attention and have been widely applied in cardiovascular research. The use of NP-DDS in computed tomography has been demonstrated to be helpful for detecting the macrophage-rich arterial walls in animal models (18) and is being tested in clinical trials (19). In addition, nanoscale contrast enhancers for magnetic resonance imaging have been applied to imaging of the formation process of atherosclerotic lesions and myocardial infarction (20-22). A number of studies have tested NP-DDS as an effective strategy for therapeutic neovascularization in clinical limb ischemia (7,23), pulmonary artery hypertension (6,24), vein graft disease (25), ischemia-reperfusion injury (26) and coronary stents (9,27). These studies have confirmed that P-NP at a 100 to 840-fold lower single dose appears to be as effective as a cumulative systemic dose of pitavastatin (6,7). The properties of NP-DDS may be the result of two major mechanisms: i) Recognition and incorporation by the mononuclear phagocyte system (monocytes, macrophages and neutrophils), which may affect the blood circulation time and tissue/cell distribution of drugs delivered by the NP-DDS; and ii) enhanced vascular permeability contributing to enhanced drug delivery for atherosclerotic arterial walls and macrophages (28). In the present study, FITC-NP was still detected in the atherosclerotic plaque 7 days after a single administration, leading to the conclusion that FITC-NP may be recognized and incorporated by macrophages. The NP-DDS is likely retained in the macrophage cytoplasm for a prolonged period (≥7 days), with the encapsulated drug being slowly released as the NPs are degraded in the macrophages. This suggested that the persistence of NP-DDS in the macrophages of plaques might serve an important role in the treatment of atherosclerosis. In the present study, the mice in the P-IV and P-NP groups received the same concentration of pitavastatin by intravenous injection and P-NP; however, the treatment effects were stronger in the P-NP group compared with those in the P-IV group. This suggested that delivering pitavastatin using an NP-DDS might increase its effectiveness.

Macrophages have been recognized as crucial components of atherosclerotic initiation and progression (29). In addition, macrophage foam cell formation reflects the disruption of the homeostatic mechanism that controls the uptake, intracellular metabolism and efflux of cholesterol within macrophages (30). SR-A1 and ACAT-1 are the key enzymes of uptake and intracellular metabolism of cholesterol within macrophages (30). Adjustment of these enzymes may be used to inhibit macrophage foam cell formation as a means of treating atherosclerosis. Studies have demonstrated that statins attenuate macrophage foam cell formation as a result of regulating cholesterol metabolism within macrophages (31). Inflammation is responsible for the initiation and progression of atherosclerosis; MCP-1 recruits monocytes to migrate to the subendothelial membrane, and M-CSF is the main facilitator that induces monocyte differentiation into macrophages. MCP-1 and M-CSF are proinflammatory factors that serve important roles in the pathogenesis of atherosclerosis (30). Statins are considered to reduce cardiovascular morbidity and mortality

through anti-inflammatory effects (32). An important finding of the present study was that weekly intravenous administration of P-NP in small doses significantly attenuated the development of atherosclerotic plaques. The plaque area was the smallest in the P-NP group compared with the other groups, which may have been associated with the significantly lower levels of SR-A1, ACAT-1 and inflammatory factors (MCP-1 and M-CSF). The *in vitro* results further confirmed that P-NP significantly reduced the levels of SR-A1, ACAT-1, IL-6 and TNF-α. These results suggested that the advantage of anti-atherosclerosis treatment by P-NP may partly be the result of the intensive adjustment of key cholesterol metabolism enzymes and the anti-inflammatory action of P-NP. The lipid levels (TG, TC, LDL-C and HDL-C) were not significantly lower in the P-NP group compared with the other intervention groups (including P-IV and P-Oral groups), suggesting that the advantages of the P-NP treatment may be independent of its lipid-lowering effect. The results of the present study suggested that NP-mediated delivery of pitavastatin promoted plaque stability, which was consistent with a previously published study (33); however, the research methods and established mechanisms were not identical. Therefore, the beneficial effects of P-NP on atherosclerosis may be attributable to the pleiotropic effects of pitavastatin, independent of its lipid-lowering effect, including the inhibition of the key enzymes of cholesterol metabolism and inflammation.

The present study evaluated whether a small dose of P-NP may be superior to a large oral dose of pitavastatin in preventing the progression of atherosclerosis. The results demonstrated that weekly administration of 0.4 mg/kg P-NP intravenously for 12 weeks significantly decelerated the progression of atherosclerosis and increased the stability of the atheromatous plaques, the effect of small doses P-NP on atherosclerosis is as large or larger than daily oral large dose of pitavastatin (1 mg/kg for 84 days). The cumulative effect of intravenous P-NP appeared to be as effective at a ≥17.5-fold in oral pitavastatin. Additionally, the ALT level was significantly lower in the P-NP group compared with the P-Oral group, indicating that P-NP is safer compared with pitavastatin alone.

In conclusion, the results of the present study demonstrated that the use of an NP-DDS for the delivery of pitavastatin appeared to have advantages in attenuating the progression of atherosclerosis and improving the stability of plaques compared with pitavastatin alone. The present results may be limited by species and research period. Despite certain limitations, the present study indicated that NP-mediated delivery of pitavastatin may exert favorable effects in patients with atherosclerosis. In summary, NP-mediated delivery of pitavastatin may provide a new targeting agent that is more feasible, effective and safer for the treatment of atherosclerotic plaques. The present study provided experimental evidence to support potential clinical applications. However, further research is needed to confirm whether P-NP may be safer and more effective in treating arteriosclerosis compared with pitavastatin alone.

Availability of data and materials

The datasets used and/or analyzed during the present study are available from the corresponding author on reasonable request.

Authors' contributions

YJS performed most experiments and analyzed the data, and was a major contributor in designing and writing the manuscript. LC and SJZ performed the animal experiments. LYS performed the cell experiments. HL collected and analyzed the data. WT analyzed and reviewed the results. GXQ made substantial contributions to conception and design of the study and revised the manuscript. All authors read and approved the final manuscript.

Ethics approval and consent to participate

The study was approved by The Institutional Animal Care and Use Committee (IACUC issue no. 2019211), China Medical University. The study followed internationally recognized guidelines on animal welfare, as well as local and national regulations.

Patient consent for publication

Not applicable.

Competing interests

The authors declare that they have no competing interests.

References

1. Baigent C, Keech A, Kearney PM, Blackwell L, Buck G, Pollicino C, Kirby A, Sourjina T, Peto R, Collins R, *et al*: Efficacy and safety of cholesterol-lowering treatment: Prospective meta-analysis of data from 90,056 participants in 14 randomised trials of statins. Lancet 366: 1267-1278, 2005.
2. Kawashiri MA, Yamagishi M, Sakamoto T, Takayama T, Hiro T, Daida H, Hirayama A, Saito S, Yamaguchi T, Matsuzaki M and COSMOS Investigators: Impact of intensive lipid lowering on lipid profiles over time and tolerability in stable coronary artery disease: Insights from a subanalysis of the coronary atherosclerosis study measuring effects of rosuvastatin using intravascular ultrasound in Japanese subjects (COSMOS). Cardiovasc Ther 31: 335-343, 2013.
3. Wakabayashi K, Nozue T, Yamamoto S, Tohyama S, Fukui K, Umezawa S, Onishi Y, Kunishima T, Sato A, Miyake S, *et al*: Efficacy of statin therapy in inducing coronary plaque regression in patients with low baseline cholesterol levels. J Atheroscler Thromb 23: 1055-1066, 2016.
4. Nissen SE, Nicholls SJ, Sipahi I, Libby P, Raichlen JS, Ballantyne CM, Davignon J, Erbel R, Fruchart JC, Tardif JC, *et al*: Effect of very high-intensity statin therapy on regression of coronary atherosclerosis: The ASTEROID trial. JAMA 295: 1556-1565, 2006.
5. Matoba T and Egashira K: Nanoparticle-mediated drug delivery system for cardiovascular disease. Int Heart J 55: 281-286, 2014.
6. Chen L, Nakano K, Kimura S, Matoba T, Iwata E, Miyagawa M, Tsujimoto H, Nagaoka K, Kishimoto J, Sunagawa K and Egashira K: Nanoparticle-mediated delivery of pitavastatin into lungs ameliorates the development and induces regression of monocrotaline-induced pulmonary artery hypertension. Hypertension 57: 343-350, 2011.
7. Kubo M, Egashira K, Inoue T, Koga J, Oda S, Chen L, Nakano K, Matoba T, Kawashima Y, Hara K, *et al*: Therapeutic neovascularization by nanotechnology-mediated cell-selective delivery of pitavastatin into the vascular endothelium. Arterioscler Thromb Vasc Biol 29: 796-801, 2009.
8. Oda S, Nagahama R, Nakano K, Matoba T, Kubo M, Sunagawa K, Tominaga R and Egashira K: Nanoparticle-mediated endothelial cell-selective delivery of pitavastatin induces functional collateral arteries (therapeutic arteriogenesis) in a rabbit model of chronic hind limb ischemia. J Vasc Surg 52: 412-420, 2010.
9. Tsukie N, Nakano K, Matoba T, Masuda S, Iwata E, Miyagawa M, Zhao G, Meng W, Kishimoto J, Sunagawa K and Egashira K: Pitavastatin-incorporated nanoparticle-eluting stents attenuate in-stent stenosis without delayed endothelial healing effects in a porcine coronary artery model. J Atheroscler Thromb 20: 32-45, 2013.
10. Starr T, Bauler TJ, Malik-Kale P and Steele-Mortimer O: The phorbol 12-myristate- 13-acetate differentiation protocol is critical to the interaction of THP-1 macrophages with Salmonella Typhimurium. PLoS One 13: e0193601, 2018.
11. Livak KJ and Schmittgen TD: Analysis of relative gene expression data using real-time quantitative PCR and the 2(-Delta Delta C(T)) method. Methods 25: 402-408, 2001.
12. Daley JM, Thomay AA, Connolly MD, Reichner JS and Albina JE: Use of Ly6G-specific monoclonal antibody to deplete neutrophils in mice. J Leukoc Biol 83: 64-70, 2008.
13. Lee PY, Wang JX, Parisini E, Dascher CC and Nigrovic PA: Ly6 family proteins in neutrophil biology. J Leukoc Biol 94: 585-594, 2013.
14. Leuschner F, Dutta P, Gorbatov R, Novobrantseva TI, Donahoe JS, Courties G, Lee KM, Kim JI, Markmann JF, Marinelli B, *et al*: Therapeutic siRNA silencing in inflammatory monocytes in mice. Nat Biotechnol 29: 1005-1010, 2011.
15. Banfi C, Baetta R, Gianazza E and Tremoli E: Technological advances and proteomic applications in drug discovery and target deconvolution: Identification of the pleiotropic effects of statins. Drug Discov Today 22: 848-869, 2017.
16. Helin-Salmivaara A, Lavikainen PT, Korhonen MJ, Halava H, Martikainen JE, Saastamoinen LK, Virta L, Klaukka T and Huupponen R: Pattern of statin use among 10 cohorts of new users from 1995 to 2004: A register-based nationwide study. Am J Manag Care 16: 116-122, 2010.
17. Jackevicius CA, Mamdani M and Tu JV: Adherence with statin therapy in elderly patients with and without acute coronary syndromes. JAMA 288: 462-467, 2002.
18. Bhavane R, Badea C, Ghaghada KB, Clark D, Vela D, Moturu A, Annapragada A, Johnson GA, Willerson JT and Annapragada A: Dual-energy computed tomography imaging of atherosclerotic plaques in a mouse model using a liposomal-iodine nanoparticle contrast agent. Circ Cardiovasc Imaging 6: 285-294, 2013.
19. Weissleder R, Nahrendorf M and Pittet MJ: Imaging macrophages with nanoparticles. Nat Mater 13: 125-138, 2014.
20. Mulder WJ and Fayad ZA: Nanomedicine captures cardiovascular disease. Arterioscler Thromb Vasc Biol 28: 801-802, 2008.
21. Leuschner F and Nahrendorf M: Molecular imaging of coronary atherosclerosis and myocardial infarction: Considerations for the bench and perspectives for the clinic. Circ Res 108: 593-606, 2011.
22. Michalska M, Machtoub L, Manthey HD, Bauer E, Herold V, Krohne G, Lykowsky G, Hildenbrand M, Kampf T, Jakob P, *et al*: Visualization of vascular inflammation in the atherosclerotic mouse by ultrasmall superparamagnetic iron oxide vascular cell adhesion molecule-1-specific nanoparticles. Arterioscler Thromb Vasc Biol 32: 2350-2357, 2012.
23. Nagahama R, Matoba T, Nakano K, Kim-Mitsuyama S, Sunagawa K and Egashira K: Nanoparticle-mediated delivery of pioglitazone enhances therapeutic neovascularization in a murine model of hindlimb ischemia. Arterioscler Thromb Vasc Biol 32: 2427-2434, 2012.
24. Kimura S, Egashira K, Chen L, Nakano K, Iwata E, Miyagawa M, Tsujimoto H, Hara K, Morishita R, Sueishi K, *et al*: Nanoparticle-mediated delivery of nuclear factor kappaB decoy into lungs ameliorates monocrotaline-induced pulmonary arterial hypertension. Hypertension 53: 877-883, 2009.

25. Kimura S, Egashira K, Nakano K, Iwata E, Miyagawa M, Tsujimoto H, Hara K, Kawashima Y, Tominaga R and Sunagawa K: Local delivery of imatinib mesylate (STI571)-incorporated nanoparticle ex vivo suppresses vein graft neointima formation. Circulation 118(14 Suppl): S65-S70, 2008.

26. Nagaoka K, Matoba T, Mao Y, Nakano Y, Ikeda G, Egusa S, Tokutome M, Nagahama R, Nakano K, Sunagawa K and Egashira K: A new therapeutic modality for acute myocardial infarction: Nanoparticle-mediated delivery of pitavastatin induces cardioprotection from ischemia-reperfusion injury via activation of PI3K/Akt pathway and anti-inflammation in a rat model. PLoS One 10: e0132451, 2015.

27. Nakano K, Egashira K, Masuda S, Funakoshi K, Zhao G, Kimura S, Matoba T, Sueishi K, Endo Y, Kawashima Y, et al: Formulation of nanoparticle-eluting stents by a cationic electro-deposition coating technology: Efficient nano-drug delivery via bioabsorbable polymeric nanoparticle-eluting stents in porcine coronary arteries. JACC Cardiovasc Interv 2: 277-283, 2009.

28. Matoba T, Koga JI, Nakano K, Egashira K and Tsutsui H: Nanoparticle-mediated drug delivery system for atherosclerotic cardiovascular disease. J Cardiol 70: 206-211, 2017.

29. Zhang W, Yancey PG, Su YR, Babaev VR, Zhang Y, Fazio S and Linton MF: Inactivation of macrophage scavenger receptor class B type I promotes atherosclerotic lesion development in apolipoprotein E-deficient mice. Circulation 108: 2258-2263, 2003.

30. McLaren JE, Michael DR, Ashlin TG and Ramji DP: Cytokines, macrophage lipid metabolism and foam cells: Implications for cardiovascular disease therapy. Prog Lipid Res 50: 331-347, 2011.

31. Leon C, Hill JS and Wasan KM: Potential role of acyl-coenzyme A: Cholesterol transferase (ACAT) inhibitors as hypolipidemic and antiatherosclerosis drugs. Pharm Res 22: 1578-1588, 2005.

32. Berman JP, Farkouh ME and Rosenson RS: Emerging anti-inflammatory drugs for atherosclerosis. Expert Opin Emerg Drugs 18: 193-205, 2013.

33. Katsuki S, Matoba T, Nakashiro S, Sato K, Koga J, Nakano K, Nakano Y, Egusa S, Sunagawa K and Egashira K: Nanoparticle-mediated delivery of pitavastatin inhibits atherosclerotic plaque destabilization/rupture in mice by regulating the recruitment of inflammatory monocytes. Circulation 129: 896-906, 2014.